This manuscript was accepted and published by ***Energy & Fuels***, a journal of the American Chemical Society. 10.1021/ef101079r (http://dx.doi.org/10.1021/ef101079r).

This manuscript was placed into the present public repository with the consent of the Editor of *Energy & Fuels*. The publication data of the final, corrected work are:

Várhegyi, G.; Bobály, B.; Jakab, E.; Chen, H.: Thermogravimetric study of biomass pyrolysis kinetics. A distributed activation energy model with prediction tests. *Energy Fuels*, **2011**, 25, 24-32. doi: 10.1021/ef101079r

Thermogravimetric study of biomass pyrolysis kinetics. A distributed activation energy model with prediction tests

Gábor Várhegyi,[†,] Balázs Bobály,[†] Emma Jakab,[†] and Honggang Chen,[‡]*

[†] Institute of Materials and Environmental Chemistry, Chemical Research Center, Hungarian Academy of Sciences, P.O. Box 17, Budapest, Hungary 1525; and [‡] National Engineering Laboratory for Biomass Power Generation Equipment, School of Renewable Energy, North China Electric Power University, 2 Beinong Road, Beijing, China 102206

[*] To whom correspondence should be addressed.

E-mail: varhegyi.gabor@ttk.mta.hu, Tel. +36 1 4381148, Fax: +36 1 4381147

ABSTRACT. The pyrolysis of four biomasses (corn stalk, rice husk, sorghum straw and wheat straw) was studied at different temperature – time functions in inert gas flow by thermogravimetric analysis (TGA). Linear and stepwise heating programs were employed. A distributed activation energy model (DAEM) with three pools of reactant (three pseudocomponents) was used due to the complexity of the biomass samples of agricultural origin. Compensation effects were observed between the kinetic parameters similarly to the works of other investigators. The compensation effects result in ambiguous parameter values hence they were eliminated by decreasing the number of the unknown parameters. For this purpose part of the kinetic parameters was assumed to be the same for the four biomasses. This approach also helps to express the similarities of the samples in the model. The sixteen experiments were evaluated simultaneously by the method of least squares to obtain dependable kinetic parameters.

The resulting models described well the experimental data and were suitable for predicting experiments at higher heating rates. The checks on the prediction capabilities were considered to be an essential part of the model verification.

Keywords: Corn stalk; rice husk; sorghum; wheat straw; thermal decomposition; kinetics; prediction.

1. Introduction

There is a growing interest in biomass fuels and raw materials due to climatic change problems. The thermal decomposition reactions play a crucial role during several of the biomass utilization processes. Thermogravimetric analysis (TGA) is a high-precision method for the study of the pyrolysis at low heating rates, under well defined conditions in the kinetic regime. It can provide information on the partial processes and reaction kinetics. On the other hand, TGA can be employed only at relatively low heating rates because the true temperature of the samples may become unknown at high heating rates.

TGA has frequently been employed in the kinetic modeling of the thermal degradation of biomass materials. Due to the complex composition of biomass materials, the conventional linearization techniques of the non-isothermal kinetics are not suitable for the evaluation of the TGA experiments. Therefore the TGA experiments of biomass materials are usually evaluated by the non-linear method of least squares (LSQ), assuming more than one reaction.[1-18]

The biomass fuels and raw materials contain a wide variety of pyrolyzing species. Even the same chemical species may have different reactivity if their pyrolysis is influenced by other species in their vicinity. The assumption of a distribution on the reactivity of the species frequently helps in the kinetic evaluation of the pyrolysis of complex organic samples.[19] The distributed reactivity is usually approximated by a Gaussian distribution of the activation energy, though other approaches are also available.[19] Distributed activation energy models (DAEM) have been used for biomass pyrolysis kinetics since 1985, when Avni et al. applied a DAEM for the formation of volatiles from lignin.[20]

Later this type of research was extended to a wider range of biomasses and materials derived from plants, including several studies on tobacco devolatilization.[21-32]

Despite the complicated mathematics of this type of modeling, the works based on DAEM kinetics have frequently employed more than one parallel reaction. The resolution of the overlapping curves by parallel DAEM reactions and the finding of a good fit were achieved by a trial-and-error parameter-search in several studies.[24,25,28,33] Burnham et al. reported a versatile computer software in 1987 that was capable for the determination of the unknown model parameters by nonlinear regression.[34] The same software was also able to determine discrete, empirical distribution functions for the activation energy during the evaluation of non-isothermal experiments.

Holstein et al.[35] and de Jong et al.[28] reported a strong compensation effect between the parameters of the Gaussian DAEM. As de Jong et al.[28] wrote: "... it is more advantageous to fit A, E_0, and σ values to experimental data using a trial-and error approach. Non-unique solutions are usually found as a result of this fitting procedure, which is due to the so-called compensation effect. In other words, different pairs of kinetic parameters provide an equally good fit to experimental data. For this reason, the values of pre-exponential factors are often fixed, and selected ... so that they are consistent with the transition-state theory ($A \approx 10^{11}$–10^{16} s^{-1})." The ill-conditioned behavior of the DAEM model was confirmed by other investigations, too. For example, a ca. 10% change in E_0 can be well compensated by a proper change of the corresponding distribution width and pre-exponential factor.[31]

Várhegyi et al.[23,31-32] and Becidan et al.[29] based DAEM kinetic studies on the simultaneous evaluation of experiments with linear and stepwise temperature programs. This method served to increase the available experimental information, as outlined elsewhere.[36] The increase of the information content of the experiments is particularly important when overlapping processes are described by parallel DAEM reactions. The determination of the unknown model parameters and the verification of the model were based on the least-squares evaluation of series of experiments. This approach led to favorable results and allowed predictions outside the experimental conditions of the experiments used in the parameter

determination.[23,29] The prediction capabilities were checked as a test on the goodness of the employed models.

In a recent article on pyrolysis kinetics, Várhegyi et al. assumed identical means ($E_{0,j}$) and distribution widths ($\sigma_{0,j}$) for the activation energies of different biomasses in a DAEM with two pseudocomponents.[30] This approach emphasized the similarities between the studied samples and decreased the problems of ill-conditioning mentioned above. The experimental part of this study was limited to linear heating programs. In a more detailed study Várhegyi et al. systematically investigated the effects of assuming common kinetic parameters for two tobaccos at linear and non-linear temperature programs.[31]

The present work stepped further in the above directions. Various assumptions of common kinetic parameters were tested on four biomasses at linear and non-linear temperature programs. The goodness of the models was judged both by the quality of fit and by their ability for predictions. The latter was considered as a stricter criterion. Experiments of slow heating were used to predict the pyrolysis behavior at a considerably higher heating rate and the predictions were compared to actual experiments. Such modeling / evaluation strategy was searched that produced good results in the prediction tests. Model variants producing rougher approximations were also considered if they offer additional advantages.

2. Samples and Methods

2.1. Samples. Corn stalk, rice husk, sorghum straw and wheat straw samples were obtained from the Shandong Shanxian Biomass Power Plant.[37] The samples were used as received. They consisted of ca. 0.1 – 3 mm particles. The larger particles were oblong in the straws and flat in the other samples. The moisture content of the samples was between 5 and 6% m/m. These values, however, are irrelevant in thermogravimetic studies, because the samples dry completely before the start of the thermal decomposition reactions. The rest of the analytical data are summarized in Table 1. As Table 1 shows, the ash content varied between 4 and 16 percent. The other analytical characteristics, however,

exhibited only low or moderate variations. Future work is planned to test the methods and considerations of the present paper on biomasses varying in wider ranges.

Table 1. Analytical Characteristics of the Samples[a]

	corn stalk	rice husk	sorghum straw	wheat straw
ash / % (db)	12.1	16.0	4.4	8.1
C / % (daf)	47.2	49.2	46.1	46.8
H / % (daf)	7.0	5.3	5.8	7.3
N / % (daf)	1.1	0.7	0.7	0.6
S / % (daf)	0.3	0.2	0.1	0.4
O / % (daf)	44.4	44.6	47.3	45.0
Ash composition data (% m/m):				
Al	1.2	0.6	1.0	1.5
Ca	4.0	1.4	5.7	3.6
Fe	0.7	0.4	0.7	0.7
K	32.6	13.6	28.0	26.3
Mg	2.6	2.2	3.6	1.5
Mn	0.0	0.1	0.1	0.1
Na	0.7	0.7	0.9	4.8
P	1.0	4.4	1.4	0.2
S	2.4	0.8	2.6	3.7
Si	16.3	32.3	17.2	19.3

[a] The ash was prepared by CEN/TS 14775 standard. *db* and *daf* stand for dry and dry ash free basis, respectively. The ash analysis was carried out by ICP-OES method on 19 elements of which the components with concentration above 0.1% are shown.

2.2. Thermogravimetric experiments. The TGA measurements were performed by a computerized Perkin-Elmer TGS-2 thermobalance in a gas flow of argon. Low initial sample masses (1 – 4 mg) were used to avoid the thermal lag problems in the biomass during the pyrolysis. The samples were spread in

a platinum sample pan of ∅ 6 mm. The apparatus was purged with the carrier gas for 45 min before starting the heating programs. The experimental curves were normalized by their sample mass value after the drying section. For this purpose the value at 120°C was used. Two linear heating programs with heating rates 4 and 40 °C/min and two stepwise heating programs were employed for each sample to increase the amount of information in the series of experiments, as mentioned above. Figure 1 shows the normalized mass-loss-rates (-d*m*/dt) of the samples at 40 °C/min heating rate. The mass loss started at 160-200°C and terminated around 600°C; hence the domain 150-600°C was selected for kinetic evaluation. The level of a considerable mass loss rate was achieved above 200°C. The slow, flat tailing of the -d*m*/dt peak in the upper part of the T domain was considered less interesting than the main decomposition steps. On this basis stepwise heating programs were defined that contained isothermal sections of 25 minutes between 225 to 400 °C, as shown in Figure 2a. The rice husk sample evidenced a small side peak around 240°C, as shown in Figure 1. Around 450°C, after the main peak, the mass loss rate was higher than those of the other samples although the main peak itself was the lowest at this sample. For these reasons a slightly wider domain was selected for the isothermal steps of the rice husk experiments, as displayed in Figure 2b. The initial sample mass was 1 and 4 mg in the experiments with 40 and 4°C/min heating rates, respectively, while 2 mg was employed at stepwise T(t).

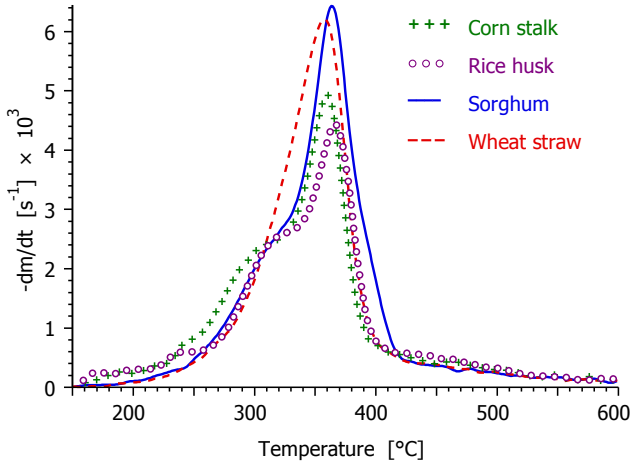

Figure 1. Mass-loss rate curves normalized by the initial dry sample mass at 40 °C/min heating rate.

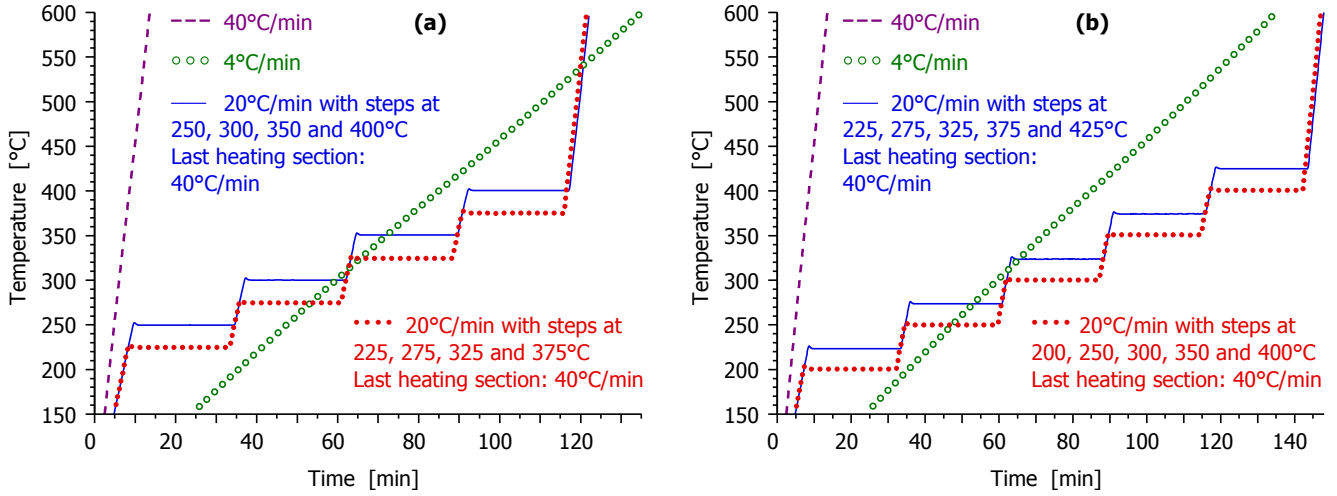

Figure 2. Temperature programs for the corn stalk, sorghum straw and wheat straw samples (a) and for the rice husk sample (b).

2.3. Evaluation by the method of least squares. The unknown model parameters were evaluated from series of experiments by minimizing the difference between the observed data and their counterparts calculated from the given model:

$$S_N = \sum_{k=1}^{N} \sum_{i=1}^{N_k} \frac{\left[\left(\frac{dm}{dt} \right)_k^{obs} (t_i) - \left(\frac{dm}{dt} \right)_k^{calc} (t_i) \right]^2}{N_k h_k^{\,2}} \qquad (1)$$

Here N is the number of experiments in the evaluated series. Subscript k indicates the different experiments. t_i denotes the time values in which the discrete experimental values were taken, and N_k is the number of the t_i points in a given experiment. h_k denotes the heights of the evaluated curves that strongly depend on the experimental conditions. The division by h_k^2 serves for normalization. The quality of the fit was characterized by the following quantity:

$$fit_N\,(\%) = 100\ S_N^{0.5} \qquad (2)$$

Equations 1 and 2 can be employed to express the quality of the fit for any group within the evaluated experiments. When the fit quality is calculated for one experiment, $S_1^{0.5}$ equals to the normalized root mean square (rms) deviation of the calculated data from the observations.

2.4. Distributed activation energy model (DAEM). As outlined in the *Introduction,* a model of parallel reactions with Gaussian activation energy distribution was chosen due to the favorable experience with this type of modeling on similarly complex materials. According to this model the sample is regarded as a sum of M pseudocomponents, where M is between 2 and 4.[23-25,28-2929,31,33,35] Here a pseudocomponent is the totality of those decomposing species which can be described by the same reaction kinetic parameters in the given model. The number of reacting species is obviously much higher than M in a complicated mixture of plant materials. The reactivity differences are described by different activation energy values. On a molecular level each species in pseudocomponent j is assumed to undergo a first-order decay. The corresponding rate constant (k) and mean lifetime (τ) are supposed to depend on the temperature by an Arrhenius formula:

$$k(T) = \tau^{-1} = A_j e^{-E/RT} \tag{3}$$

Let $\alpha_j(t,E)$ be the solution of the corresponding first order kinetic equation at a given E and $T(t)$ with conditions $\alpha_j(0,E)=0$ and $\alpha_j(\infty,E)=1$:

$$d\alpha_j(t,E)/dt = A_j e^{-E/RT} [1-\alpha_j(t,E)] \tag{4}$$

The density function of the species differing by E within a given pseudocomponent is denoted by $D_j(E)$. $D_j(E)$ is approximated by a Gaussian distribution with mean $E_{0,j}$ and width-parameter (variation) σ_j. The overall reacted fraction of the jth pseudocomponent, $\alpha_j(t)$ is obtained by integration:

$$\alpha_j(t) = \int_0^\infty D_j(E)\ \alpha_j(t,E)\ dE \tag{5}$$

The normalized sample mass, m, and its derivative are the linear combinations of $\alpha_j(t)$ and $d\alpha_j/dt$, respectively:

$$-dm/dt = \sum_{j=1}^{M} c_j d\alpha_j / dt \quad \text{and} \quad m(t) = 1 - \sum_{j=1}^{M} c_j \alpha_j(t) \tag{6}$$

where a weight factor c_j is equal to the amount of volatiles formed from a unit mass of pseudocomponent j.

2.5. Numerical methods. The software (Fortran 95 and C++ programs) was developed by one of the authors and has already been used in earlier work.[23,29-32]. The applied algorithms were described in details in a recent article.[31]

3. Results and discussion

3.1. About the magnitudes of the observed reaction rates. As described above, four common biomasses of agricultural origin were studied at linear and stepwise temperature programs. Table 2 shows the highest and the average reaction rates observed at the four heating programs. The averaging was carried out in the temperature domain of the kinetic evaluation, from 150 to 600 °C. Table 2 serves to estimate the extent of extrapolation in the prediction tests outlined in Section 3.5 In these tests the 40°C/min experiments are predicted from the slower experiments. As the data of Table 2 shows, this procedure is an extrapolation to 4 – 11 times higher reaction rates.

Table 2. The highest and mean normalized mass loss rates ($-dm/dt \times 10^3 / s^{-1}$) in the experiments[a]

Experiment	corn stalk		rice husk		sorghum straw		wheat straw	
	peak	mean	peak	mean	peak	mean	peak	mean
4 °C/min	0.59	0.010	0.49	0.010	0.66	0.011	0.67	0.011
Stepwise 1	0.62	0.009	0.93	0.008	1.07	0.011	0.86	0.010
Stepwise 2	1.09	0.010	0.73	0.008	1.14	0.011	1.42	0.010
40 °C/min	4.94	0.103	4.44	0.098	6.43	0.115	6.21	0.110

[a] The means were calculated in the temperature domain of the kinetic evaluation, from 150 to 600 °C. Heating programs "Stepwise 1" and "Stepwise 2" are shown in Figure 2 by blue solid lines and red dotted lines, respectively.

3.2. The necessary number of pseudocomponents. The biomasses contain a wide variety of decomposing species and the catalytic activity of the inorganic ions increases further this diversity. This complexity is described by a distributed activation energy model with more than one pseudocomponent (pool of reactant), as outlined in the Introduction and in Section 2.4. At 40°C/min heating rate the mass

loss rate curves of corn stalk, rice husk and sorghum straw reveal a main peak around 360 °C and a side peak around 300 °C. (See Figure 1). These peaks can be attributed to the cellulose and hemicellulose decomposition, respectively.[38] The two peaks are highly merged in the case of the wheat straw. The merging of the cellulose and hemicellulose peaks can probably be due to the catalytic activities of the mineral content.[38] As a first step, the evaluation was tried with the assumption of two pseudocomponents, of which the first described the hemicelluloses and cellulose pyrolysis and the second covered the other decomposition reactions. The corresponding simulated curves however, could not mimic the double peaks shown in Figure 1. For this reason the number of pseudocomponents was increased to 3. The chemical aspects of the three pseudocomponents will be briefly discussed in Section 3.6.

3.3. Separate evaluation of the samples. In evaluation I each sample was assumed to have its own parameters: $E_{0,j}$, σ_j, A_j and c_j (j=1, 2, 3). Accordingly 4×3×4=48 parameters were needed for the description of the experiments on the four samples. In this case the number of experiments evaluated simultaneously (N in eq 1) was 4 for each sample. Column I of Table 3 shows an overview of the corresponding results. The first value, fit_{16}, represents the quality of the fit for the whole series of experiments. The quality of the fit of the four 40°C/min experiments, $fit_{40°C/min}$, was also calculated for a comparison with the results of the prediction tests of Section 3.5. The kinetic parameters will be discussed in Section 3.6.

3.4. Assumption of common parameters. In the next step of the work the 16 experiments were evaluated simultaneously by the method of least squares to obtain dependable kinetic parameters. Part of the parameters was assumed to be the same for the four biomasses. This approach helps to emphasize the similarities of the samples and eliminate the ill-conditioning of the parameter determination that was mentioned in the Introduction. In Evaluation II the mean activation energies, $E_{0,j}$ were assumed to be identical for the different biomasses. This approach only slightly changed the quality of the fit, while the parameter estimation became better defined due to the lower number of unknown parameters. (See Section 3.5.) The quality of the fit and the partial curves at 40°C/min heating rate are illustrated in the

left side of Figure 3. The full version of this figure with all the 16 experiments can be found in the *Supporting Information*, alongside with the electronic version of this article.

Table 3. Comparison of the results of the model variants employed[a]

Evaluation	I	II	III	IV	V
Identical parameters	none	$E_{0,j}$	$E_{0,j}$, σ_j	$E_{0,j}$, A_j	$E_{0,j}$, σ_j, A_j
fit_{16} / %	1.8	1.9	2.2	3.0	3.6
$fit_{40°C/min}$ / %	1.8	1.9	2.5	3.4	4.1
$E_{0,1}$ / kJ mol^{-1}	<173>	176	177	178	176
$E_{0,2}$ / kJ mol^{-1}	<186>	185	185	185	185
$E_{0,3}$ / kJ mol^{-1}	<205>	195	194	192	189
σ_1 / kJ mol^{-1}	<5.5>	<5.5>	4.3	<4.5>	7.1
σ_2 / kJ mol^{-1}	<1.1>	<1.1>	1.9	<1.3>	1.7
σ_3 / kJ mol^{-1}	<35.7>	<33.8>	34.5	<34.2>	32.7
$\log_{10} A_1$ / s^{-1}	<13.96>	<14.21>	<14.43>	14.41	14.13
$\log_{10} A_2$ / s^{-1}	<13.83>	<13.77>	<13.77>	13.75	13.71
$\log_{10} A_3$ / s^{-1}	<14.91>	<14.19>	<14.23>	14.23	13.90
c_1	<0.15>	<0.14>	<0.10>	<0.11>	<0.12>
c_2	<0.31>	<0.31>	<0.33>	<0.31>	<0.31>
c_3	<0.26>	<0.27>	<0.29>	<0.30>	<0.29>
$N_{parameters}$	48	39	30	30	21
$N_{parameters}/N$	3.0	2.4	1.9	1.9	1.3
Characteristics of the partial peaks simulated at 40°C/min[b]					
$T_{peak,1}$ / °C	296 – 336	295 – 335	294 – 317	307 – 314	312
$T_{peak,2}$ / °C	360 – 366	360 – 366	359 – 368	361 – 363	363
$T_{peak,3}$ / °C	353 – 401	352 – 397	350 – 379	359	361
$FWHM_1$ / °C	43 – 91	44 – 88	49 – 52	38 – 90	69
$FWHM_2$ / °C	42 – 51	42 – 52	45 – 47	43 – 49	46
$FWHM_3$ / °C	250 – 271	250 – 273	260 – 272	175 – 316	257

[a] Brackets < > indicate average values. Hyphens indicate intervals. FWHM stands for full width at half maximum

[b] The listed peak characteristics belong to simulations at ideal (error-free) *T(t)* programs with $dT/dt \equiv 2/3$ °C/s (40 °C/min).

In Evaluation III $E_{0,j}$ and σ_j were assumed to be identical for the different biomasses. The quality of the fit slightly worsened; fit_{16} increased from 1.9 to 2.2 %. In this approximation: the compositional differences in the biomasses and the different catalytic effects were expressed by the different c_j and A_j values. One should emphasize here that the larger part of the experimental errors are not statistical in thermal analysis. Hence no statistical background is available to assess the statistical significance of a change in the quality of the fit.[36] The two other variations, Evaluations IV and V resulted in visibly worse fit qualities than Evaluations I-III. Nevertheless, Evaluation V may have practical advantages in numerical simulations: all structural and compositional differences are expressed by the c_j parameters in this case. Note that the solution of the model, *m(t)* and $-dm/dt$ depend linearly on c_j. This might involve practical advantages: the adjustment of the model to a changed feedstock is particularly simple in this model variant. Among others the mixing of various biomass components can be expressed by the mixing of their simulated *m(t)* and $-dm/dt$ functions in this approximation at any *T(t)*. The quality of the fit and the partial curves of evaluation V are illustrated at 40°C/min heating rate in the left side of Figure 4. The full version of this figure with all the 16 experiments can be found in the *Supporting Information*. In this approximation the model provides the same calculated partial peaks (thin solid lines of blue, red and dark green colors) at a given temperature program; only their multiplier factors (c_j) depend on the biomass properties. Accordingly the peak temperatures ($T_{peak,j}$) and peak widths ($FWHM_j$) in Table 3 do not depend on the biomass properties in this case. The parameters and peak characteristics of evaluations II and V are listed in Table 4.

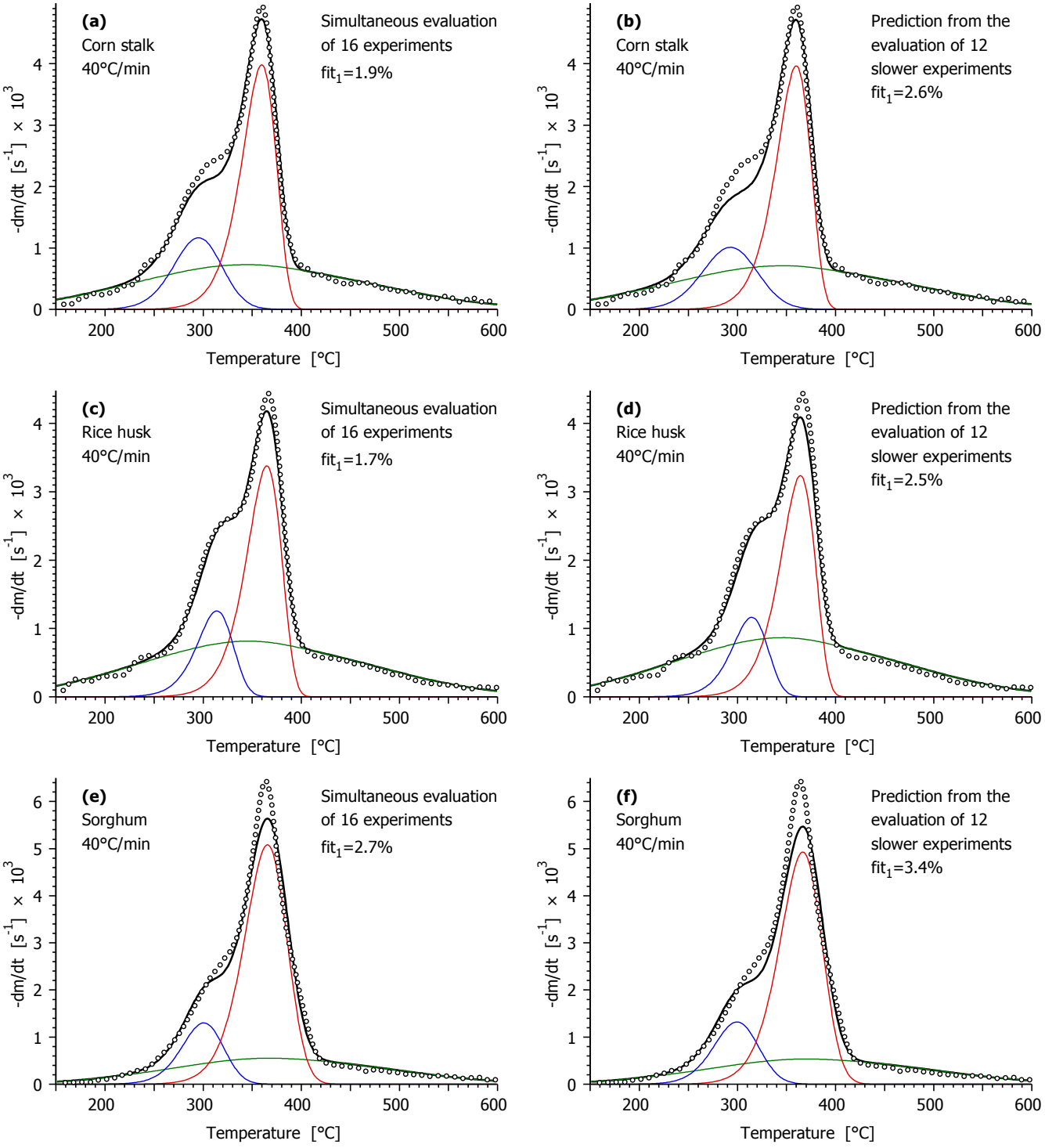

Figure 3. Results for the 40°C/min experiments in Evaluation II. The experimental data (○○○), their simulated counterparts (**—**) and the calculated partial curves (blue, red and green —) are displayed. The left hand side (Parts **a**, **c**, **e**, **g**) illustrates the simultaneous evaluation of all available experiments. The right hand side (Parts **b**, **d**, **f**, **h**) shows the prediction of the 40°C/min experiments from the evaluation of the slower experiments of the study.

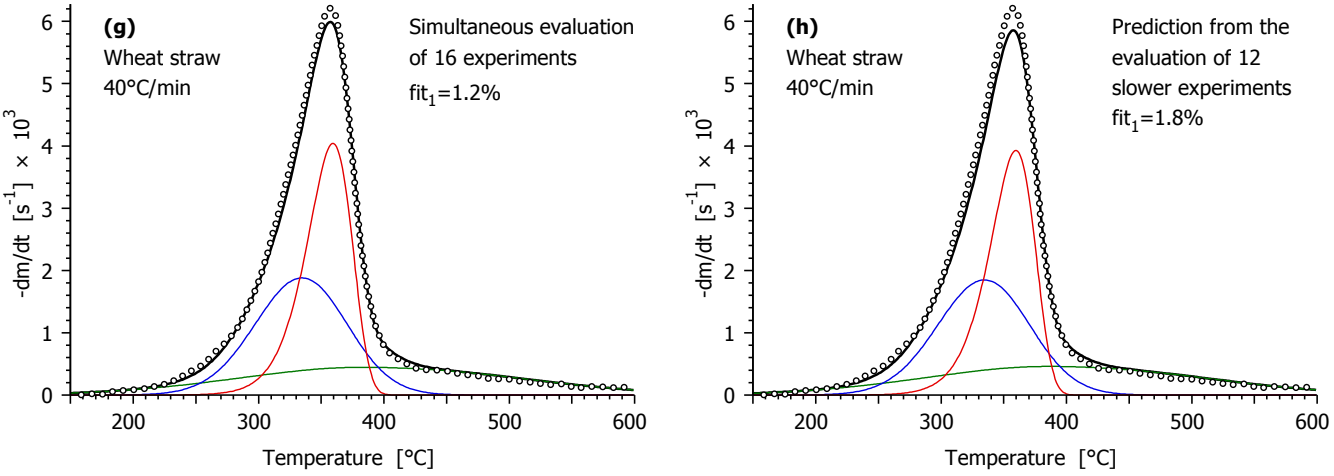

Figure 3. *(Continued)*

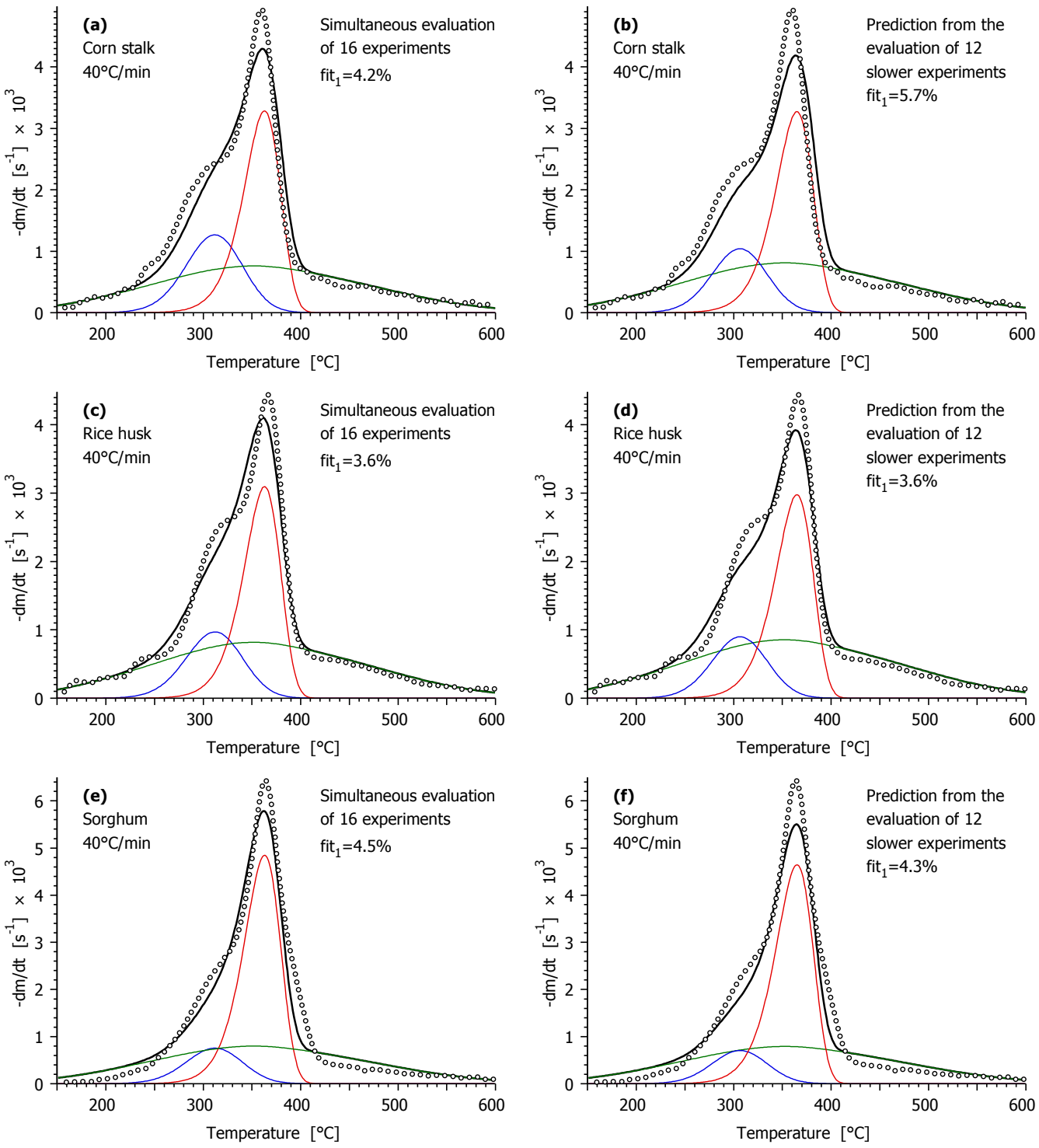

Figure 4. Results for the 40°C/min experiments in Evaluation V, when identical kinetic parameters ($E_{0,j}$, σ_j and A_j values) were assumed for the four biomasses. The experimental data (○○○), their simulated counterparts (**—**) and the calculated partial curves (blue, red and green —) are displayed. The left hand side (Parts **a**, **c**, **e**, **g**) illustrates the simultaneous evaluation of all available experiments. The right hand side (Parts **b**, **d**, **f**, **h**) shows the prediction of the 40°C/min experiments from the evaluation of the slower experiments of the study.

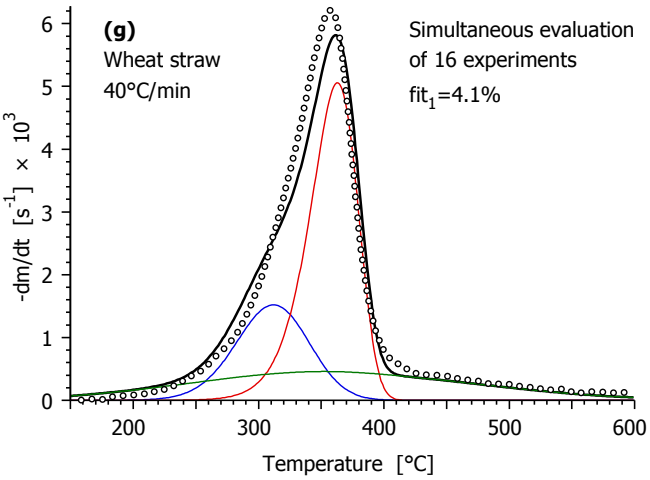

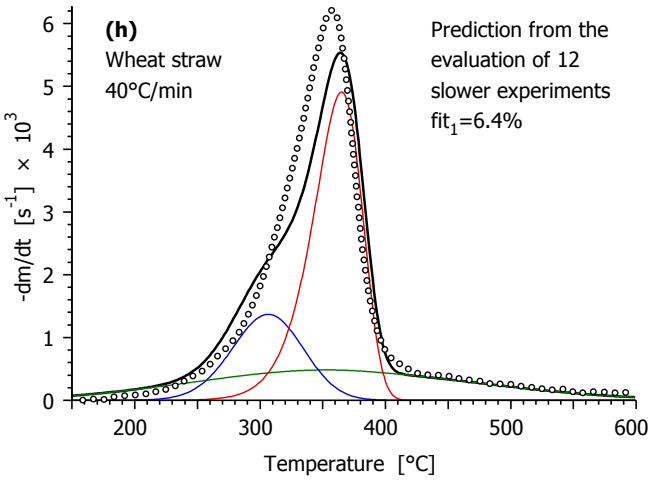

Figure 4. *(Continued)*

Table 4. Parameters and peak characteristics of Evaluations II and V.

Evaluation	II				V			
Identical parameters	$E_{0,j}$				$E_{0,j}$, σ_j, A_j			
Sample	corn stalk	rice husk	sorghum straw	wheat straw	corn stalk	rice husk	sorghum straw	wheat straw
fit_{16} / %	1.9				3.6			
$fit_{40°C/min}$ / %	2.2	2.0	1.9	1.3	3.8	2.9	4.2	3.3
$E_{0,1}$ / kJ mol^{-1}	176				176			
$E_{0,2}$ / kJ mol^{-1}	185				185			
$E_{0,3}$ / kJ mol^{-1}	195				189			
σ_1 / kJ mol^{-1}	5.8	2.5	4.3	9.4	7.1			
σ_2 / kJ mol^{-1}	0.0	0.0	3.5	1.0	1.7			
σ_3 / kJ mol^{-1}	36.6	35.6	32.0	31.2	32.7			
$\log_{10} A_1$ / s^{-1}	14.64	14.19	14.52	13.48	14.13			
$\log_{10} A_2$ / s^{-1}	13.86	13.73	13.64	13.86	13.71			
$\log_{10} A_3$ / s^{-1}	14.68	14.63	13.98	13.53	13.90			
c_1	0.11	0.09	0.10	0.26	0.14	0.10	0.08	0.16
c_2	0.28	0.24	0.44	0.29	0.25	0.23	0.36	0.38
c_3	0.32	0.35	0.22	0.19	0.31	0.34	0.33	0.19
Characteristics of the partial peaks at 40°C/min[a]*:*								
$T_{peak,1}$	295	314	300	335	312			
$T_{peak,2}$	360	365	366	360	363			
$T_{peak,3}$	352	354	379	397	361			
$FWHM_1$	58	44	50	88	69			
$FWHM_2$	42	43	52	43	46			
$FWHM_3$	273	267	250	252	257			

[a] Here the peak characteristics belong to simulations at ideal (error-free) *T(t)* programs with $dT/dt \equiv 2/3$ °C/s (40 °C/min).

3.5. Prediction of the fastest experiments from the evaluation of the experiments of 4°C/min and stepwise *T(t)*. In these tests the 12 slower experiments were evaluated in the same way as the whole series (16 experiments) and theoretical $-\mathrm{d}m/\mathrm{d}t$ curves were determined for the 40°C/min experiments. This procedure corresponds to an extrapolation to considerably higher heating rates from a given data set, as outlined in Section 3.1. The fit quality of the extrapolated curves, $fit_{40°C/min}$, is obviously worse than in the case of the regular evaluation of all the 16 experiments. However, the difference between the $fit_{40°C/min}$ values of the prediction and the corresponding regular evaluation, $\Delta fit_{40°C/min}$ has moderate values, as shown in Table 5. Table 5 also displays the differences between the parameters obtained from the slower experiments and from the whole data sets.

According to the data in Table 5, Evaluation II gives the best prediction performance; $fit_{40°C/min}$ and $\Delta fit_{40°C/min}$ are the lowest here. Figure 3 shows the fit quality of the predicted 40°C/min experiments. In the case of Evaluation II the kinetic parameters calculated from the subset of the 12 slow experiments and from all the 16 experiments are practically equivalent: the $rms(\Delta E_{0,j})$, $rms(\Delta \sigma_j)$, $rms(\Delta \log_{10} A_j)$ and $rms(\Delta c_j)$ values are negligible, indicating that the 12 slower experiments are enough for the determination of the parameters. This observation demonstrates that the parameters are mathematically well-defined (i.e. unambiguous) in the evaluation of the experiments. Evaluation I (i.e. the separate evaluation of the samples) produced worse prediction fit quality, $fit_{40°C/min}$, than Evaluation II. In this case the differences between the parameters obtained from 12 and 16 experiments are much higher than the corresponding values of Evaluation II. This behavior can probably be due to the ill-condition of the parameter determination, as outlined in the Introduction: the information content of the experiments proved to be insufficient for the unambiguous determination of 48 unknown parameters. A further decrease of the number of parameters resulted in poorer prediction ability and higher differences between the parameters obtained from 12 and 16 experiments. Accordingly, the assumptions used in these variants reduced the performance of the model. As Table 5 shows, Evaluation II is the optimum among the assumptions tested. Nevertheless, Evaluation V was inspected in details due to its computational advantages outlined in Section 3.4. Figure 4 illustrates its performance in the prediction

tests. The comparison of the corresponding panels of Figures 3 and 4 shows that difference in the prediction capabilities of Evaluations II and V are visible, but not particularly high. As outlined earlier, the fit_1 values in these figures express the rms difference between the predicted and the observed values as a percent of the peak maximum. The range of fit_1 was 1.8 – 3.4 and 3.6 – 6.4 in the right-hand sides of Figures 3 and 4, respectively. Evaluation V gave the worse prediction for the wheat straw, where fit_1 was 6.4%. However, such a prediction precision is considered to be good in many areas of science and technology.

Table 5. Differences between the evaluation of the whole series and the result of the prediction tests[a]

Evaluation	I	II	III	IV	V
Identical parameters	none	$E_{0,j}$	$E_{0,j}$, σ_j	$E_{0,j}$, A_j	$E_{0,j}$, σ_j, A_j
$fit_{40°C/min}$ / %	3.2	2.6	3.2	4.0	5.1
$\Delta fit_{40°C/min}$ / %	1.4	0.7	0.8	0.7	1.0
$rms(\Delta E_{0,j})$ / kJ mol^{-1}	15	1	6	9	18
$rms(\Delta \sigma_j)$ / kJ mol^{-1}	2.0	0.5	0.8	1.1	1.1
$rms(\Delta \log_{10} A_j)$	1.5	0.1	0.6	0.8	1.8
$rms(\Delta c_j)$	0.02	0.01	0.01	0.01	0.01

[a] Here $fit_{40°C/min}$ characterizes the distance between the predicted curves and their observed counterparts in the 40°C/min experiments, and $\Delta fit_{40°C/min}$ is the difference between the $fit_{40°C/min}$ values of Tables 5 and 3. $rms(\Delta E_{0,j})$, $rms(\Delta \sigma_j)$, $rms(\Delta \log_{10} A_j)$ and $rms(\Delta c_j)$ are the root mean square differences of the parameters obtained from all experiments and from the subset of the slower experiments.

3.6. Notes on the pseudocomponents and on the magnitudes of the obtained kinetic parameters.

The chemical identification of the calculated peaks is difficult because there is a high overlap in the decomposition domains of the biomass components. The shape and position of the first (blue) and second (red) peaks in Figures 3 and 4 are similar to the partial curves of hemicelluloses and celluloses in biomass materials, respectively.[5,38,39] The third, very wide peak denoted by dark green in Figures 3 and

4 originates from the contributions of several decomposing components. Lignin has a crucial role here because it decomposes in a wide temperature range.[40] The extractive components of the plants have similarly wide decomposition curves.[41,42] Probably the hemicelluloses and the cellulose can also contribute to this partial curve though the main part of these components is described by partial curves 1 and 2, respectively. The high-temperature part of the third peak belongs mainly to the slow carbonization of the carbonaceous residues (i.e. to the formation and slow devolatilization of the charcoal).

Table 3 shows that the activation energy distribution of the second, red-colored peak is narrow; σ_2 is only 1 – 2 kJ/mol. Note that the employed DAEM is equivalent to a first order reaction at σ=0 because the Gaussian distribution is a Dirac delta function with respect to σ. Hence this reaction is near to a first order kinetics, in accordance with the earlier works showing that the cellulose pyrolysis can be approximated by first order kinetics. The $E_{0,2}$ values were found to be 185 – 186 kJ/mol, which is safely in the range of the activation energies reported for the cellulose components of biomass materials.[1-18]

On the other hand, the $E_{0,1}$ and $E_{0,3}$ values of Table 3 are considerably higher than the reported activation energies for the decomposition of hemicelluloses and lignin in studies based on first order or *n*th order kinetics.[8] One can consider here that the activation is nearly inversely proportional to the width of the DTG curves in the first order and *n*th order models at linear *T(t)*.[43] Accordingly flat, wide peaks result in low formal activation energy values. This problem does not arise in the DAEMs because DAEMs can describe wide, flat peaks with realistic magnitudes of activation energies. Table 6 compares the magnitudes of the E_0 and σ values of four recent papers on biomass employing kinetics with parallel DAEM reactions and least squares evaluation. Note that the kinetic parameters of the different studies are not directly comparable due to the different number and kind of the pseudocomponents in the different works. Hence the comparison of the magnitudes was based only on the mean and the domain of variation of the $E_{0,j}$ and σ_j values published in a given article.

Table 6. Comparison of the magnitudes of the $E_{0,j}$ and σ_j values in four recent articles on biomass pyrolysis that employed DAEM kinetics and least squares evaluation [a]

Sample	Experi-ments	Evaluated curves	Heating programs	E_0 / kJ mol^{-1}	σ / kJ mol^{-1}	Reference
Wood pellets and *miscanthus sinensis*	TGA-FTIR	FTIR	linear	<186> 136-299	<11> 2-32	de Jong et al., 2003[24]
brewer spent grains, coffee waste, fiberboard	TGA	DTG	linear, stepwise, and CRR [b]	<211> 175-236	<14> 0-33	Becidan et al., 2007[29]
Straws of cereals and Ethiopian mustard	TGA	TGA, DTG	linear	<198> 167-232	<18> 2-35	Várhegyi et al., 2009[30]
Cornstalk, rice husk, sorghum straw, wheat straw	TGA	DTG	linear and stepwise	<184> 176-195	<14> 0-37	Table 4 of the present work

[a] For this comparison the means (in angular brackets) and intervals (denoted by hyphens) were determined from all $E_{0,j}$ and σ_j values published in the given article.

[b] CRR (constant reaction rate) stands for temperature programs at which the reaction rate fluctuates around a constant level.

4. Conclusions

Four common biomasses of agricultural origin were studied by thermogravimetry at linear and stepwise temperature programs. The complexity of the thermal decomposition of these biomasses was described by three partial reactions assuming Gaussian distributions for their activation energies. Such parameters were determined that provided a good fit for the experiments at linear and stepwise heating programs for the studied samples.

Part of the kinetic parameters was assumed to be common for the four samples for two reasons:

(i) to express/explore the similarities of the decomposition of the different samples due to their similar chemical composition

(ii) to eliminate the ill-definition (compensation effect) problems by determining less parameters from the given amount of experimental data.

Five assumptions were investigated. The best results were obtained when the $E_{0,j}$ parameters were assumed to be identical for the different biomasses. Another model variant was found to be interesting due to its practical aspects. In this latter case all the kinetic parameters ($E_{0,j}$, σ_j, A_j) were assumed to be common and the differences between the biomasses are expressed only by the the area of the partial peaks, c_j . Because the model is linear for the c_j parameters, the adjustment of the model to a changed feedstock is particularly simple in this model variant. Among others, the mixing of various biomass components can be expressed by the mixing of their simulated *m(t)* and $-\mathrm{d}m/\mathrm{d}t$ functions in this approximation at any *T(t)*.

The models provided reasonable fit to the experimental data. Besides, the evaluation of a narrower subset of the experiments (the 12 slower experiments) provided similar parameters as the evaluation of the whole series of experiments. In the best case, when identical $E_{0,j}$ parameters were assumed for the different biomasses, the parameters from the slower experiments were practically the same as their counterparts determined from the whole data set. This is an indication that the evaluation of the experiments results in well-defined (i.e. unambiguous) parameters.

The obtained models proved to be suitable to predict the behavior of the samples outside of those temperature programs at which the model parameters were determined. The checks on the prediction abilities of the models corresponded to an extrapolation to 4 – 11 times higher reaction rates than the mean and peak reaction rates of the experiments used for parameter determination in the prediction tests.

Acknowledgment. The authors thank the support of the Hungarian National Research Fund (OTKA K72710 and K81959) and the Chinese – Hungarian Intergovernmental Science & Technology Cooperation Program (CHN-35/2005). The help of Dr. Zoltán May in the ICP-OES analysis is also gratefully acknowledged.

Supporting Information Available: Figures showing the partial curves and the quality of the fit on 16 experiments at Evaluations II and V. This material is available free of charge via the Internet at http://pubs.acs.org.

NOMENCLATURE

α_j	reacted fraction of a pseudocomponent (dimensionless)
A_j	pre-exponential factor (s^{-1})
c_j	normalized mass of volatiles formed from a pseudocomponent (dimensionless)
$E_{0,j}$	mean activation energy in a distributed activation energy model (kJ/mol)
fit_N	fit quality calculated for a group of N experiments by equations 1 - 2 (%)
$fit_{40°C/min}$	fit quality calculated for the 40°C/min experiments by equations 1 - 2 (%)
$FWHM$	peak width (full width of half maximum, °C)
h_k	height of an experimental curve (s^{-1})
m	normalized sample mass (dimensionless)
N	number of experiments in a given evaluation
N_k	number of evaluated data on the kth experimental curve
R	gas constant (8.3143×10^{-3} kJ mol^{-1} K^{-1})
rms	root mean square
σ_j	width parameter (variance) of the Gaussian distribution (kJ/mol)
S_N	least squares sum for N experiments (dimensionless)
t	time (s)
T	temperature (°C, K)

Subscripts:

i	digitized point on an experimental curve
j	pseudocomponent
k	experiment

REFERENCES

(1) Várhegyi, G; Antal Jr, M.J.; Székely, T.; Szabó, P. Kinetics of the thermal decomposition of cellulose, hemicellulose, and sugarcane bagasse. *Energy Fuels* **1989**, *3*, 329-335.

(2) Cozzani, V.; Petarca, L.; Tognotti, L. Devolatilization and pyrolysis of refuse derived fuels: characterization and kinetic modelling by a thermogravimetric and calorimetric approach. *Fuel* **1995**, *74*, 903-912.

(3) Caballero, J. A.; Conesa, J. A.; Font, R.; Marcilla, A. Pyrolysis Kinetics of Almond Shells and Olive Stones Considering their Organic Fractions. *J. Anal. Appl. Pyrol.* **1997,** *42*, 159-175.

(4) Teng, H.; Lin, H. C., Ho, J. A. Thermogravimetric Analysis on Global Mass Loss Kinetics of Rice Hull Pyrolysis. *Ind. Eng. Chem. Res.* **1997**, *36*, 3974-3977.

(5) Várhegyi, G; Antal Jr, M.J.; Jakab, E.; Szabó, P. Kinetic modeling of biomass pyrolysis. *J. Anal. Appl. Pyrolysis* **1997**, *42*, 73-87.

(6) Órfão, J. J. M.; Antunes, F. J. A.; Figueiredo, J. L. Pyrolysis Kinetics of Lignocellulosic Materials - 3 Independent Reactions Model. *Fuel* **1999**, *78*, 349-358.

(7) Helsen, L.; Van den Bulck, E. Kinetics of the low-temperature pyrolysis of chromated copper arsenate-treated wood. *J. Anal. Appl. Pyrolysis* **2000**, *53*, 51-79.

(8) Garcìa-Pèrez, M.; Chaala, A.; Yang, J.; Roy, C. Co-pyrolysis of sugarcane bagasse with petroleum residue. Part I: thermogravimetric analysis. *Fuel* **2001**, *80*, 1245-1258.

(9) Sørum, L.; Grønli, M.G.; Hustad, J.E. Pyrolysis characteristics and kinetics of municipal solid wastes. *Fuel* **2001**, *80*, 1217-1227.

(10) Vamvuka, D.; Pasadakis, N.; Kastanaki E. Kinetic Modeling of Coal/Agricultural By-Product Blends. *Energy Fuels* **2003**, *17*, 549 -558.

(11) Müller-Hagedorn, M; Bockhorn, H.; Krebs, L.; Müller. U. A comparative kinetic study on the pyrolysis of three different wood species. *J. Anal. Appl. Pyrolysis* **2003**, *68-69*, 231-249.

(12) Manyà, J. J.; Velo, E.; Puigjaner, L. Kinetics of biomass pyrolysis: A reformulated three-parallel-reactions model. *Ind. Eng. Chem. Res.* **2003**, *42*, 434-441.

(13) Jauhiainen, J.; Conesa, J.A.; Font, R.; Martin-Gullon, I. Kinetics of the pyrolysis and combustion of olive oil solid waste. *J. Anal. Appl. Pyrolysis* **2004**, *72*, 9-15.

(14) Mészáros, E.; Várhegyi, G.; Jakab, E.; Marosvölgyi, B. Thermogravimetric and reaction kinetic analysis of biomass samples from an energy plantation. *Energy Fuels* **2004**, *18*, 497-507.

(15)Branca, C.; Albano A.; Di Blasi, C. Critical evaluation of global mechanisms of wood devolatilization. *Thermochim. Acta* **2005**, *429*, 133-141.

(16)Gómez, C. J.; Várhegyi, G.; Puigjaner, L. Slow pyrolysis of woody residues and an herbaceous biomass crop: A kinetic study. *Ind. Eng. Chem. Res.* **2005**, *44*, 6650-6660.

(17)Skodras, G.; Grammelis, O. P.; Basinas, P.; Kakaras, E.; Sakellaropoulos, G. Pyrolysis and combustion characteristics of biomass and waste-derived feedstock. *Ind. Eng. Chem. Res.* **2006**, *45*, 3791-3799.

(18) Müller-Hagedorn, M.; Bockhorn, H. Pyrolytic Behaviour of different biomasses (angiosperms) (maize plants, straws, and wood) in low temperature pyrolysis. *J. Anal. Appl. Pyrolysis* **2007**, *79*, 136-146.

(19)Burnham, A. K.; Braun, R. L. Global kinetic analysis of complex materials. *Energy Fuels* **1999**, *13*, 1-22.

(20)Avni, E.; Coughlin, R.W.; Solomon P.R., King H.H. Mathematical modelling of lignin pyrolysis. *Fuel* **1985**, *64,* 1495-1501.

(21)Reynolds, J. G.; Burnham, A. K. Pyrolysis decomposition kinetics of cellulose-based materials by constant heating rate micropyrolysis, *Energy Fuels* **1997**, *11*, 88-97.

(22)Reynolds, J. G.; Burnham, A. K.; Wallman, P. H. Reactivity of paper residues produced by a hydrothermal pretreatment process for municipal solid wastes, *Energy Fuels* **1997**, *11*, 98-106.

(23)Várhegyi, G.; Szabó, P.; Antal, M. J., Jr.: Kinetics of charcoal devolatilization. *Energy Fuels* **2002**, *16*, 724-731.

(24)de Jong, W; Pirone, A; Wojtowicz, M. A. Pyrolysis of Miscanthus Giganteus and wood pellets: TG-FTIR analysis and reaction kinetics. *Fuel,* **2003**, *82*, 1139-1147.

(25)Wójtowicz, M. A.; Bassilakis, R.; Smith, W. W.; Chen, Y.; Carangelo, R. M. Modeling the evolution of volatile species during tobacco pyrolysis. *J. Anal. Appl. Pyrolysis*, **2003**, *66*, 235-261.

(26)Yi, S-C.; Hajaligol, M. R. Product distribution from the pyrolysis modeling of tobacco particles. *J. Anal. Appl. Pyrolysis*, **2003**, *66*, 217-234.

(27)Yi, S-C.; Hajaligol, M. R.; Jeong, S. H. The prediction of the effects of tobacco type on smoke composition from the pyrolysis modeling of tobacco shreds. *J. Anal. Appl. Pyrolysis*, **2005**, *74*, 181-192.

(28)de Jong, W.; Di Nola, G.; Venneker, B. C. H.; Spliethoff, H.; Wójtowicz, M. A. TG-FTIR pyrolysis of coal and secondary biomass fuels: Determination of pyrolysis kinetic parameters for main species and NO_x precursors, *Fuel,* **2007**, *86*, 2367-2376.

(29)Becidan, M.; Várhegyi, G.; Hustad, J. E.; Skreiberg, Ø. Thermal decomposition of biomass wastes. A kinetic study. *Ind. Eng. Chem. Res.* **2007**, *46*, 2428 - 2437.

(30)Várhegyi, G.; Chen, H.; Godoy, S. Thermal decomposition of wheat, oat, barley and *Brassica carinata* straws. A kinetic study. *Energy Fuels* **2009**, *23*, 646-652.

(31)Várhegyi, G.; Czégény, Z.; Jakab, E.; McAdam, K.; Liu, C. Tobacco pyrolysis. Kinetic evaluation of thermogravimetric – mass spectrometric experiments. *J. Anal. Appl. Pyrolysis* **2009**, *86*, 310-322.

(32)Várhegyi, G.; Czégény, Zs.; Liu, C.; McAdam, K.: Thermogravimetric analysis of tobacco combustion assuming DAEM devolatilization and empirical char-burnoff kinetics. *Ind. Eng. Chem. Res.,* **2010**, *49*, 1591-1599.

(33)Bassilakis, R.; Zhao, Y.; Solomon, P. R.; Serio, M. A. Sulfur and nitrogen evolution in the Argonne coals: Experiment and modeling, *Energy Fuels* **1993**, *7*, 710-720.

(34)Burnham, A. K.; Braun, R. L.; Gregg, H. R. Comparison of methods for measuring kerogen pyrolysis rates and fitting kinetic parameters, *Energy Fuels* **1987**, *1*, 452-458.

(35)Holstein, A. ; Bassilakis, R.; Wójtowicz, M. A.; Serio, M. A. Kinetics of methane and tar evolution during coal pyrolysis, *Proc. Comb. Inst.* **2005**, *30*, 2177-2185.

(36)Várhegyi, G. Aims and methods in non-isothermal reaction kinetics. *J. Anal. Appl. Pyrolysis* **2007**, *79*, 278-288.

(37)United Nations Framework Convention on Climate Change, Project 1032. http://cdm.unfccc.int/Projects/DB/TUEV-SUED1175012571.81 , **2010**.

(38)Várhegyi, G.; Jakab, E.; Till, F.; Székely, T.: Thermogravimetric - mass spectrometric characterization of the thermal decomposition of sunflower stem. *Energy Fuels* **1989**, *3*, 755-760.

(39)Fisher, T.; Hajaligol, M.; Waymack, B.; Kellogg, D. Pyrolysis behavior and kinetics of biomass derived materials, *J. Anal. Appl. Pyrolysis* **2002**, *62*, 331-349.

(40)Jakab, E.; Faix, O.; Till, F.; Székely, T. Thermogravimetry/mass spectrometry study of six lignins within the scope of an international round robin test, *J. Anal. Appl. Pyrolysis* 1995, *35*, 167-179.

(41)Várhegyi, G.; Grønli, M. G.; Di Blasi, C. Effects of sample origin, extraction and hot water washing on the devolatilization kinetics of chestnut wood. *Ind. Eng. Chem. Res.* **2004**, *43*, 2356-2367.

(42)Mészáros, E.; Jakab, E.; Várhegyi, G. TG/MS, Py-GC/MS and THM-GC/MS study of the composition and thermal behavior of extractive components of *Robinia pseudoacacia*. *J. Anal. Appl. Pyrolysis* **2007**, *79,* 61-70.

(43)Várhegyi, G.; Székely, T. Reaction kinetics in thermal analysis: The sensitivity of kinetic equations to experimental errors. A mathematical analysis. *Thermochim. Acta* **1982**, *57*, 13-28.